From Aggregates to Clusters. Facile Formation of Hetero-Metal−Metal Bonds through Reductive Desulfurization by CO in a Decapacitative Transformation of a $\{Pt_2MS_2\}$ Tbp Frame to a $\{Pt_2MS\}$ Tetrahedral Core (M = Ag, Cu, and Ru)

Huang Liu,[†] Agnes L. Tan,[‡] K. F. Mok,*[,†] Thomas C. W. Mak,[§] Andrei S. Batsanov,[⊥] Judith A. K. Howard,[⊥] and T. S. Andy Hor*[,†]

Contribution from the Departments of Chemistry and Computational Science, Faculty of Science, National University of Singapore, Kent Ridge, Singapore 119260, the Department of Chemistry, The Chinese University of Hong Kong, Shatin, N. T., Hong Kong, and the Department of Chemistry, University of Durham, Durham DH1 3LE, U.K.

Received June 5, 1997[⊗]

Abstract: $[Pt_2(PPh_3)_4(\mu\text{-}S)_2]$ (**1**) reacts with $AgCl(PPh_3)$ and CuCl under a mild pressure of CO (60 psi) to give $[Pt_2(CO)(PPh_3)_3(\mu_3\text{-}S)MCl]$ [M = Ag (**4**) and Cu (**6**)] via the intermediates $[Pt_2(PPh_3)_4(\mu_3\text{-}S)_2Ag(PPh_3)]Cl$ (**2a**), $[Pt_2(PPh_3)_5(\mu_3\text{-}S)_2AgCl]$ (**3**), and $[Pt_2(PPh_3)_5(\mu_3\text{-}S)_2CuCl]$ (**5**), respectively. These transformations demonstrate an unprecedented concomitant process which involve heterometalation, carbonylation, reductive desulfurization, and metal−metal bond formation. The Ru−Pt aggregate of $[Pt_2(PPh_3)_4(\mu_3\text{-}S)_2RuCl(PPh_3)_2]Cl$ (**7**), prepared from **1** and $RuCl_2(PPh_3)_3$, similarly converts to a $[Pt_2(CO)_2(PPh_3)_2(\mu_3\text{-}S)RuCl(CO)(PPh_3)]Cl$ (**8**) cluster under a CO atmosphere. Such transformation establishes a synthetic relationship between the $\{Pt_2MS_2\}$ trigonal bipyramidal aggregates and $\{Pt_2MS\}$ tetrahedral clusters and provides a general entry to triangular heterometallic sulfide clusters of platinum. All complexes are characterized by IR, $^{31}P\{^1H\}$, and ^{13}C NMR spectroscopy and conductivity measurements. The structures of **4**, **6**, and the PF_6^- derivative of **2a** (*viz*. **2b**) have also been determined by single-crystal X-ray diffraction analyses. The structure of **2b** shows a sulfide-bicapped Ag−Pt mixed-metal triangle without significant Pt···Pt [3.351(2) and 3.375(2) Å] or Ag···Pt [av 3.064(1) and 3.101(1) Å] interactions. Complex **2b** crystallizes in two polymorphic modifications with different degrees of disposition of the Ag moieties with respect to the $\{Pt_2S_2\}$ core. As a result, the Ag−S bonds [2.479(1) *vs* 2.585(1) Å and 2.502(2) *vs* 2.607(2) Å] are significantly different between the polymorphs in which the Ag···Pt distances are near-equivalent [3.061(1) *vs* 3.066(1) Å] in one form but significantly different [2.962(1) *vs* 3.240(1) Å] in the other. Complex **4** shows a triangular $\{AgPt_2\}$ cluster mono-capped by sulfide. Removal of a capping sulfur atom from **2a** effectively reduces both Pt^{II} centers and favors Pt−Pt bond formation [Pt−Pt 2.658(2) Å] and heterometallic Ag−Pt interactions [av Ag−Pt 2.965(1) Å] in **4**. Both the Pt−S and Ag−S bonds also strengthen significantly from **2b** to **4**. Cluster **6** is isostructural to **4** with similar homo- [Pt−Pt 2.657(1) Å] and heterometal [av Cu−Pt 2.832(1) Å interactions. Both **4** and **6** thus constitute a $\{MPt_2S\}$ distorted tetrahedral cluster frame. A facile and general aggregates-to-clusters conversion through the elimination of COS gas is thus established.

Introduction

The use of $[Pt_2(PPh_3)_4(\mu\text{-}S)_2]$ (**1**) as a precursor to homo-,[1] hetero-,[2] and intermetallic[3] sulfide complexes offers a powerful means in the design of mixed-metal materials. By using this strategy, a variety of polynuclear complexes with nuclearities ranging from three to six in all common geometries have been constructed.[1−3] Since virtually any metal compounds with some Lewis acidic character can be incorporated to the $\{Pt_2S_2\}$ core, the generality and versatility of this method are unmatched by most other established routes in heteromultimetallic syntheses.[4] Among the materials isolated, the metal−metal separations are almost invariably outside the bonding distances for most metals. This is hardly surprising as these complexes are based on a $\{Pt_2S_2\}$ butterfly core containing two 16-electron square-planar Pt^{II} centers. Such lack of active metal−metal bonds in a polynuclear architecture, which prompted Mingos to describe them as "aggregates"[2c] (as opposed to "clusters"), prevents the metals from undergoing a closer (electrochemical[5]) com-

[†] Department of Chemistry, National University of Singapore.
[‡] Department of Computational Science, National University of Singapore.
[§] The Chinese University of Hong Kong.
[⊥] University of Durham.
[⊗] Abstract published in *Advance ACS Abstracts,* October 15, 1997.

(1) Aw, B. H.; Looh, K. K.; Chan, H. S. O.; Tan, K. L.; Hor, T. S. A. *J. Chem. Soc., Dalton Trans.* **1994**, 3177.

(2) (a) Briant, C. E.; Hor, T. S. A.; Howells, N. D.; Mingos, D. M. P. *J. Chem. Soc., Chem. Commun.* **1983**, 1118. (b) Briant, C. E.; Hor, T. S. A.; Howells, N. D.; Mingos, D. M. P. *J. Organomet. Chem.* **1983**, *256*, C15. (c) Briant, C. E.; Gilmour, D. I.; Luke, M. A.; Mingos, D. M. P. *J. Chem. Soc., Dalton Trans.* **1985**, 851. (d) Bos, W.; Bour, J. J.; Schlebos, P. P. J.; Hageman, P.; Bosman, W. P.; Smits, J. M. M.; Van Wietmarschen, J. A. C.; Beurskens, P. T. *Inorg. Chim Acta* **1986**, *119*, 141. (e) Gilmour, D. I.; Luke, M. A.; Mingos, D. M. P. *J. Chem. Soc., Dalton Trans.* **1987**, 335. (f) Liu, H.; Tan, A. L.; Mok, K. F.; Hor, T. S. A. *J. Chem. Soc., Dalton Trans.* **1996**, 4023. (g) Liu, H.; Tan, A. L.; Xu, Y.; Mok, K. F.; Hor, T. S. A. *Polyhedron* **1997**, *16*, 377. (h) Liu, H.; Tan, A. L.; Cheng, C. R.; Mok, K. F.; Hor, T. S. A. *Inorg. Chem.* **1997**, *36*, 2916.

(3) (a) Zhou, M.; Xu, Y.; Koh, L.-L.; Mok, K. F.; Leung, P.-H.; Hor, T. S. A. *Inorg. Chem.* **1993**, *32*, 1875. (b) Zhou, M.; Xu, Y.; Lam, C.-F.; Koh, L.-L.; Mok, K. F.; Leung, P.-H.; Hor, T. S. A. *Inorg. Chem.* **1993**, *32*, 4660. (c) Zhou, M.; Xu, Y.; Lam, C.-F.; Leung, P.-H.; Koh, L.-L.; Mok, K. F.; Hor, T. S. A. *Inorg. Chem.* **1994**, *33*, 1572.

(4) (a) Hor, T. S. A. *J. Cluster Sci.* **1996**, *7*, 263. (b) Richter, F.; Vahrenkamp, H. *Angew. Chem., Int. Ed. Engl.* **1978**, *17*, 444. (c) Adams, R. D.; Hor, T. S. A. *Inorg. Chem.* **1984**, *23*, 4723. (d) Adams, R. D.; Pompeo, M. P.; Wu, W. *Inorg. Chem.* **1991**, *30*, 2899. (e) Kuwata, S.; Mizobe, Y.; Hidai, M. *J. Am. Chem. Soc.* **1993**, *115*, 8499.

(5) Zhou, M.; Xu, Y.; Tan, A.-M.; Leung, P.-H.; Mok, K. F.; Koh, L.-L.; Hor, T. S. A. *Inorg. Chem.* **1995**, *34*, 6425.

S0002-7863(97)01837-4 CCC: $14.00

Scheme 1

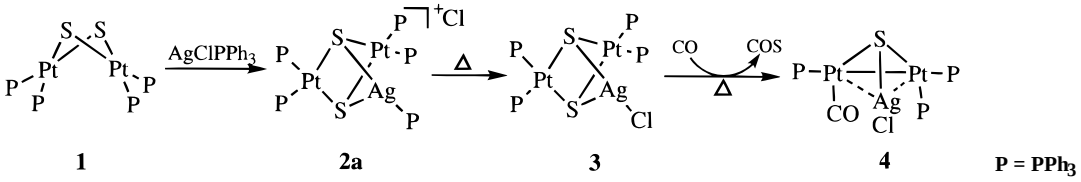

1 **2a** **3** **4**

munication and (catalytic[2e]) cooperation. Our objective is therefore to devise a pathway for transforming these aggregates into metal clusters. In view of the abundance of hetero- and intermetallic aggregates thus found, such conversion would pave a simple and unprecedented entry to heterometallic platinum clusters[4a] which are surprisingly lacking among the wide-spread occurrence of metal sulfide clusters.[6]

The use of reduction as a strategy to generate the metal−metal bond is an established concept. However, there is no simple means to convert a $\{M_3S_2\}$ aggregate to a $\{M_3S\}$ cluster without causing cluster degradation, nuclearity expansion, or ligand transformation. All the common reducing agents (*e.g.* Zn, Na/Hg, BH_4^-, N_2H_4, BuLi, *etc.*) have poor selectivities and specificities. In this paper we report a simple use of CO gas as a reducing and desulfurizing agent. The efficiency of the conversion is demonstrated in the synthesis of a series of heterometallic sulfide clusters, such as $[Pt_2(CO)(PPh_3)_3(\mu_3\text{-}S)MCl]$ [M = Ag (**4**); Cu (**6**)] and $[Pt_2(CO)_2(PPh_3)_2(\mu_3\text{-}S)RuCl(CO)(PPh_3)]Cl$ (**8**) from **1** via the aggregates, such as $[Pt_2(PPh_3)_4(\mu_3\text{-}S)_2Ag(PPh_3)]Cl$ (**2a**), $[Pt_2(PPh_3)_4(\mu_3\text{-}S)_2AgCl]$ (**3**), $[Pt_2(PPh_3)_4(\mu_3\text{-}S)_2CuCl]$ (**5**), and $[Pt_2(PPh_3)_4(\mu_3\text{-}S)_2RuCl(PPh_3)_2]Cl$ (**7**), respectively. The isolation and characterization of these intermediates illustrate the general significance of this carbonylative desulfurization approach to metal−metal bond formation.

Results and Discussion

Preparation of $[Pt_2(CO)(PPh_3)_3(\mu_3\text{-}S)AgCl]$ (4). A mixture of **1** and $AgCl(PPh_3)$ (1:1) under a mild CO atmosphere (60 psi) in an autoclave at 80 °C gives **4**. The Pt−carbonyl absorption (2025 cm^{-1}) in **4** is significantly higher than that in $Pt^I_2(CO)(PPh_3)_3(\mu\text{-}S)$ (ν_{CO} 1998 cm^{-1}).[7] This is consistent with the expected electron drift away from the Pt_2 moiety upon S → Ag bond formation. The $^{31}P\{^1H\}$ NMR spectrum of **4** shows three inequivalent phosphines with associated ^{195}Pt satellites, but no Ag phosphine is apparent. The conductivity measurement indicates it to be a non-electrolyte.

We have previously reported the formation of $[Pt_2(PPh_3)_4(\mu_3\text{-}S)_2AgCl]$ (**3**) from **1** via $[Pt_2(PPh_3)_4(\mu_3\text{-}S)_2Ag(PPh_3)]Cl$ (**2a**) in air.[2h] To verify that **2a** is an active intermediate in the formation of **4** from **1** under CO, we have isolated **2a** and investigated its reaction with CO in an autoclave. The conversion from aggregate **2a** to cluster **4** is verified by both IR and $^{31}P\{^1H\}$ NMR analysis of the isolated product (Scheme 1).

In the process of the cluster formation, carbon monoxide gas plays a unique and multifunctional role. Besides being a ligand as commonly known, it induces the formation of Pt−Pt and Ag−Pt bonds by an unusual reductive desulfurization process. No Ph_3PS was detected in the reaction mixture whereas the elimination of sulfide in the form of COS was observed. A similar desulfurization process was noted in the conversion of **1** to $Pt_2(CO)_n(PPh_3)_{4-n}(\mu\text{-}S)$ ($n = 1-3$).[7c] This signifies a reverse of the well-known oxidative cleavage of COS as a source for CO and sulfur in metal complexes.[7,8] The ability of CO to facilitate a selective desulfurization process (instead of a blanket removal of all the sulfur atoms as demonstrated by other strong sulfur scavengers) and partial reduction (instead of harsh reduction from Pt(II) to Pt(0) and/or Ag(I) to Ag(0), e.g., by $NaBH_4$ or N_2H_4) helps to preserve the cluster framework and offers an advantage to the use of CO. The easy removal of the byproduct provides an additional incentive. There is no other common reagent that can fulfil such a multitasking role with such efficiency.

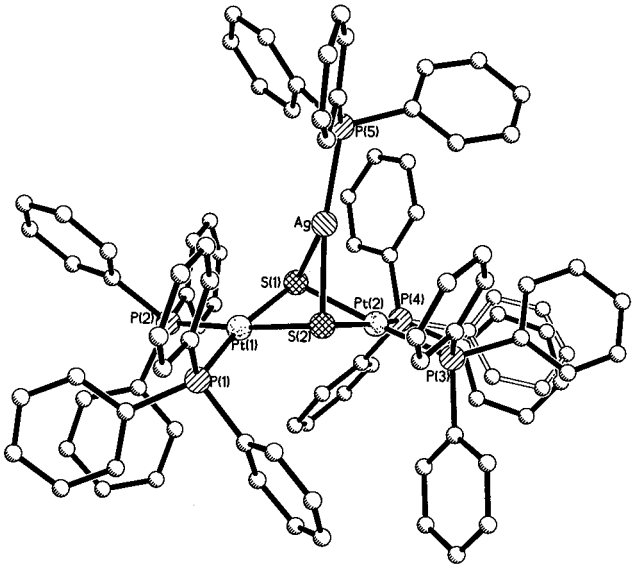

Figure 1. The structure of a polymorphic form of $[Pt_2(PPh_3)_4(\mu_3\text{-}S)_2Ag(PPh_3)]PF_6$, **2b**(**B**).

Crystal Structures of 4 and the PF_6^- Derivative (2b) of Intermediate 2a. The structures of **4** and the PF_6^- derivative (**2b**) of intermediate **2a** have been determined by their single-crystal X-ray diffraction analyses.

Complex **2b** crystallizes in two polymorphic modifications with the space group of $P2_12_12_1$ for **2b**(**A**) and $P\bar{1}$ for **2b**(**B**). Both structural forms show a sulfide-bicapped $\{AgPt_2\}$ triangle (Figure 1), but some of their bonding parameters, especially the M···M separations, are significantly different (Table 1). The two Ag···Pt separations are essentially identical in one modification [3.061(1) *vs* 3.066(1) Å] but significantly different in the other [2.962(1) *vs* 3.240(1) Å]. In both forms, the Ag fragment is asymmetrically disposed with respect to the sulfide [2.479(1) and 2.585(1) Å in **2b**(**A**) and 2.502(2) and 2.607(2) Å in **2b**(**B**)]. No metal orbital interaction is expected between the 16-electron metal fragments [av Ag−Pt 3.064(1) and 3.101(1) Å], although some electrostatic interactions cannot be ignored. The Pt···Pt separation [3.351(2) and 3.35(2) Å] is typically nonbonding. The local geometry of the Ag atom is best described as "Y-shaped", with an acute S(1)−Ag−S(2) bite

(6) (a) Dance, I.; Fisher, K. *Prog. Inorg. Chem.* **1994**, *41*, 637. (b) Pasynskii, A. A.; Eremenklo, I. L. *Russ. Chem. Rev.* **1989**, *58*, 181. (c) Shibahara, T. *Adv. Inorg. Chem.* **1991**, *37*, 143. (d) Holm, R. H. *Adv. Inorg. Chem.* **1992**, *38*, 1. (e) Adams, R. D. *Polyhedron* **1985**, *4*, 2003.

(7) (a) Baird, M. C.; Wilkinson, G. *J. Chem. Soc. A* **1967**, 865. (b) Evans, D. G.; Hallam, M. F.; Mingos, D. M. P.; Wardle, R. W. M. *J. Chem. Soc., Dalton Trans.* **1987**, 1889. (c) Chin, C.-H.; Hor, T. S. A. *J. Organomet. Chem.* **1996**, *509*, 101.

(8) Hallam, M.; Luke, M. A.; Mingos, D. M. P.; Williams, I. D. *J. Organomet. Chem.* **1987**, *325*, 271.

Table 1. Selected Bond Lengths (Å) and Angles (deg) in $[Pt_2(PPh_3)_4(\mu_3\text{-}S)_2Ag(PPh_3)]PF_6$ (**2b**)

	Polymorph **A**		
Pt(1)−S(1)	2.353(1)	Pt(1)−S(2)	2.371(1)
Pt(2)−S(1)	2.366(1)	Pt(2)−S(2)	2.348(1)
Ag−S(1)	2.479(1)	Ag−S(2)	2.585(1)
Pt(1)−P(1)	2.285(1)	Pt(1)−P(2)	2.307(1)
Pt(2)−P(3)	2.294(1)	Pt(2)−P(4)	2.284(1)
Ag−P(5)	2.327(1)	Ag···Pt(1)	3.061(1)
Ag···Pt(2)	3.066(1)	Pt(1)···Pt(2)	3.351(2)
Pt(1)−S(1)−Pt(2)	90.49(3)	Pt(1)−S(1)−Ag	78.56(3)
Pt(1)−S(2)−Pt(2)	90.50(3)	Pt(1)−S(2)−Ag	76.14(3)
Pt(2)−S(1)−Ag	78.48(3)	Pt(2)−S(2)−Ag	76.69(3)
S(1)−Pt(1)−S(2)	82.70(3)	S(1)−Pt(2)−S(2)	82.90(3)
S(1)−Ag−S(2)	76.04(3)	S(1)−Ag−P(5)	146.79(3)
S(2)−Ag−P(5)	136.53(3)	P(1)−Pt(1)−S(1)	89.56(3)
P(1)−Pt(1)−S(2)	172.03(3)	P(1)−Pt(1)−P(2)	102.44(3)
P(3)−Pt(2)−S(1)	86.64(3)	P(3)−Pt(2)−S(2)	169.53(3)
P(3)−Pt(2)−P(4)	99.93(3)		
	Polymorph **B**		
Pt(1)−S(1)	2.343(2)	Pt(1)−S(2)	2.355(2)
Pt(2)−S(1)	2.369(2)	Pt(2)−S(2)	2.366(2)
Ag−S(1)	2.607(2)	Ag−S(2)	2.502(2)
Pt(1)−P(1)	2.293(2)	Pt(1)−P(2)	2.279(2)
Pt(2)−P(3)	2.298(2)	Pt(2)−P(4)	2.281(2)
Ag−P(5)	2.343(2)	Ag···Pt(1)	3.240(1)
Ag···Pt(2)	2.962(1)	Pt(1)···Pt(2)	3.375(2)
Pt(1)−S(1)−Pt(2)	91.49(7)	Pt(1)−S(1)−Ag	81.60(6)
Pt(1)−S(2)−Pt(2)	91.26(7)	Pt(1)−S(2)−Ag	83.64(6)
Pt(2)−S(1)−Ag	72.91(5)	Pt(2)−S(2)−Ag	74.92(6)
S(1)−Pt(1)−S(2)	82.15(7)	S(1)−Pt(2)−S(2)	81.38(7)
S(1)−Ag−S(2)	74.33(7)	S(1)−Ag−P(5)	135.46(8)
S(2)−Ag−P(5)	150.19(8)	P(1)−Pt(1)−S(1)	167.68(7)
P(1)−Pt(1)−S(2)	85.98(7)	P(1)−Pt(1)−P(2)	100.63(8)
P(3)−Pt(2)−S(1)	168.84(7)	P(3)−Pt(2)−S(2)	88.86(7)
P(3)−Pt(2)−P(4)	106.75(8)		

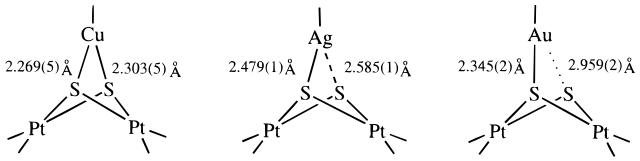

Figure 2. The M−S bond distances in $[Pt_2(PPh_3)_4(\mu_3\text{-}S)_2M(PPh_3)]^+$ (M = Cu, Ag, and Au) showing the increasing differences between the two M−S bonds upon descending the group.

angle [76.04(3)° and 74.33(7)°] and two significantly larger P(5)−Ag−S angles [146.79(3)° and 150.19(8)°, and 136.53(3)° and 135.36(8)°]. Similar Y-shaped geometry has been found in its Cu analogue of $[Pt_2(PPh_3)_4(\mu_3\text{-}S)_2Cu(PPh_3)]PF_6$[2g] but not in the Au counterpart $[Pt_2(PPh_3)_4(\mu\text{-}S)(\mu_3\text{-}S)Au(PPh_3)]NO_3\cdot 0.5H_2O$.[2d] In the latter complex, the Au atom adopts a distorted linear geometry. The preference of lower coordination for the heavier congener in group 11 complexes is evident (Figure 2).

The core structure of **4** is shown in Figure 3. In the conversion from **2a** to **4**, the sulfide-bicapped Ag−Pt triangle (or a $\{Pt_2AgS_2\}$ tbp) undergoes a "decapitation" to give a monosulfide-capped metal triangle (or a $\{Pt_2AgS\}$ tetrahedron) thus effectively reducing both Pt^{II} centers to formally Pt^{I}, which favors Pt−Pt bond formation. As a result, the Pt−Pt bond shortens significantly from 3.351(2) and 3.375(2) Å in **2b** to 2.658(2) Å in **4** (Table 2). The latter length is similar to that in other Pt^{I}−Pt^{I} bonded species {*e.g.* $[Pt_2(CO)(PPh_3)_3(\mu\text{-}S)]$[7] [2.647(2) Å] and $[Pt_2(CO))(PPh_3)_3(\mu_3\text{-}S)Au(PPh_3)]PF_6$ [8][2.649(2) Å]}. The reduced charge on both Pt atoms also promotes some heterometallic Ag−Pt interactions {the av Ag−Pt 2.965(1) Å is significantly shorter than those in **2b**}. With a nearly linear S(1)−Ag(1)−Cl(1) angle [175.1(1)°], the geometry of the Ag atom in **4** is distorted tetrahedral, which is contrary to the "Y-shaped" geometry in **2b**. Phosphine displacement by CO occurs at one of the Pt^{I} spheres; this is indicative of better stabilization of a reduced metal by a stronger π-acceptor. The multifunctional role of CO as a ligand, reductant, and sulfur scavenger is thus evident.

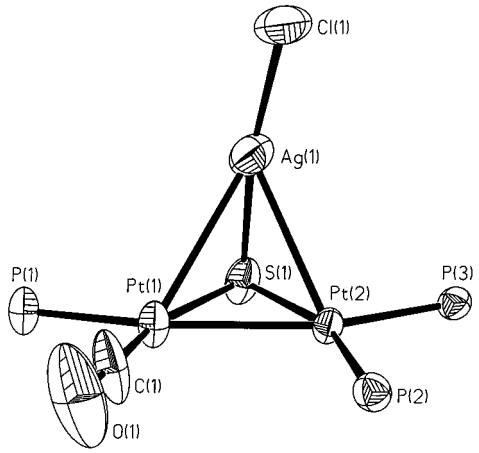

Figure 3. An ORTEP plot of $[Pt_2(CO)(PPh_3)_3(\mu_3\text{-}S)AgCl]$, **4**, with a 50% probability level (phenyl rings removed for clarity).

In a $\{AgPt_2\}$ metal triangle with all three metals formally in a +1 oxidation state, an interesting question arises on the existence and degree of interdependence of the Pt−Pt and Ag−Pt bonds, and how these M−M interactions affect the M−S lengths. Using a simple valence-bond model based on 16-electron Pt^{I} and 14- or 16-electron Ag^{I}, one can illustrate this delicate interrelationship (Scheme 2). Strong Ag−Pt bonds would occur at the expense of the Pt−Pt or even Ag−S bonds. Fenske−Hall MO calculations[9] of **4** (Table 3) support the concept of strong Pt−Pt and weak Ag−Pt bonds (similar to Model **III** in Scheme 2). It also shows that the Pt−Pt molecular orbital describes a measure of interaction between Pt nonbonding electrons and Ag. [For Pt−Pt along the *z*-axis, the percent character of this molecular orbital is as follows: Pt(1) $d_{x^2-y^2}$ 4.74, d_{yz} 3.58, s 7.23, p_y 1.49, p_z 10.74; Pt(2) $d_{x^2-y^2}$ 2.25, d_{yz} 6.34, s 4.91, p_y 1.37, p_z 12.69; Ag(1) s 2.32.] Indeed, if the AgCl moiety is bent toward the Pt_2S plane, the Ag−Pt interaction increases at the expense of the Ag−S bond (Table 3) (analogous to Model **IV**), and to a lesser extent the Pt−Pt bond (compared with Models **II** and **IV**).

Preparation and Crystal Structure of $[Pt_2(CO)(PPh_3)_3(\mu_3\text{-}S)CuCl]$ (6). This one-pot synthesis of clusters from aggregates is also evident in the Cu(I) system. Mixing CuCl with **1** in an autoclave under CO pressure results in a Cu−Pt cluster **6**, which is also stabilized by a carbonyl displacement of the phosphines (ν_{CO} 2026 cm^{-1}). The $^{31}P\{^{1}H\}$ NMR spectrum is similar to that of **4**. The formation of **6** via $[CuPt_2Cl(PPh_3)_4(\mu_3\text{-}S)_2]$ (**5**) is reasonable and supported by the observation that **5** can be isolated in the addition reaction of **1** with CuCl at room temperature.

The X-ray single-crystal diffraction analysis of **6** shows a sulfur-capped $\{CuPt_2\}$ triangle isostructural to **4** (Figure 4 and Table 4). The Pt−Pt bond (2.657(1) Å) is identical with that in **4**. The two Cu−Pt bond lengths [2.755(1) and 2.888(1) Å] are comparable to the weaker Cu−Pt bonds found in $[CuPt_3(PPh_3)_5(\mu\text{-}CO)_3](BF_4)$[10] [2.577(3)−2.735(3) Å]. Similar to cluster **4**, the chloride ligand is essentially *trans* to the sulfide atom [S(1)−Cu(1)−Cl(1) 175.1(1)°] in **6**, thus giving a distorted tetrahedral geometry of Cu(I). Similar distortion has been observed in $[CuPt_3(PPh_3)_5(\mu\text{-}CO)_3](BF_4)$.[10] The resultant strength

(9) Hall, M. B.; Fenske, R. F. *Inorg. Chem.* **1972**, *11*, 768.
(10) Braunstein, P.; Freyburger, S. *J. Organomet. Chem.* **1988**, *352*, C29.

Scheme 2

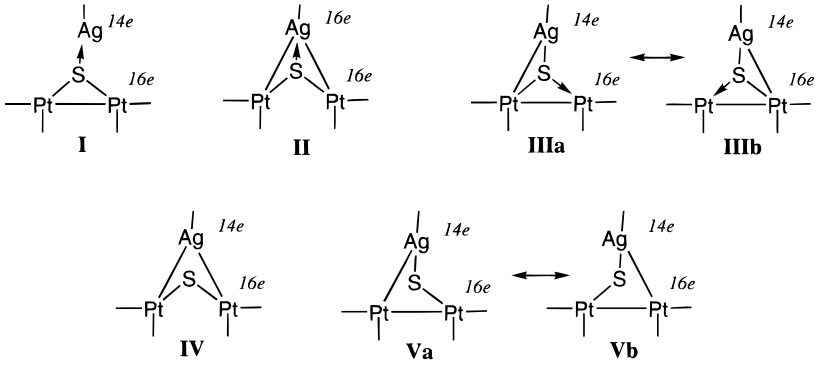

Table 2. Selected Bond Lengths (Å) and Angles (deg) in $[Pt_2(CO)(PPh_3)_3(\mu_3\text{-}S)AgCl]$ (**4**)

Pt(1)−Pt(2)	2.658(1)	Ag(1)−Pt(1)	3.024(1)
Ag(1)−Pt(2)	2.906(1)	Pt(1)−S(1)	2.279(2)
Pt(2)−S(1)	2.278(2)	Ag(1)−S(1)	2.427(3)
Pt(1)−P(1)	2.322(2)	Pt(2)−P(2)	2.258(2)
Pt(2)−P(3)	2.276(2)	Pt(1)−C(1)	1.856(10)
Ag(1)−Cl(1)	2.352(3)	C(1)−O(1)	1.120(13)
Pt(1)−Pt(2)−Ag(1)	65.7(1)	Pt(1)−Ag(1)−Pt(2)	53.2(1)
Pt(2)−Pt(1)−Ag(1)	61.1(1)	Pt(1)−Pt(2)−S(1)	54.3(1)
Pt(1)−S(1)−Pt(2)	71.4(1)	Pt(2)−Pt(1)−S(1)	54.3(1)
Pt(1)−Ag(1)−S(1)	47.9(1)	Pt(1)−S(1)−Ag(1)	79.9(1)
Ag(1)−Pt(1)−S(1)	52.2(1)	Pt(2)−Ag(1)−S(1)	49.6(1)
Pt(2)−S(1)−Ag(1)	76.2(1)	Ag(1)−Pt(2)−S(1)	54.2(1)
Pt(1)−Ag(1)−Cl(1)	134.1(1)	Pt(2)−Ag(1)−Cl(1)	123.3(1)
Cl(1)−Ag(1)−S(1)	171.5(1)	Pt(1)−Pt(2)−P(2)	103.4(1)
Pt(1)−Pt(2)−P(3)	154.3(1)	Pt(2)−Pt(1)−P(1)	157.0(1)
Pt(2)−Pt(1)−C(1)	105.0(3)	Ag(1)−Pt(1)−C(1)	118.3(4)
Ag(1)−Pt(1)−P(1)	110.1(1)	Ag(1)−Pt(2)−P(2)	122.0(1)
Ag(1)−Pt(2)−P(3)	101.2(1)	P(1)−Pt(1)−C(1)	97.9(3)
P(2)−Pt(2)−P(3)	102.2(1)	Pt(1)−C(1)−O(1)	176.8(10)

Table 3. Calculated Overlap Populations for Selected Bonds in Complex $[Pt_2(CO)(PPh_3)_3(\mu_3\text{-}S)AgCl]$ (**4**) [The Angles Refer to Pt(1)−S(1)−Ag(1)]

angle	normal (79.9°)	70°	90°
Pt(1)-Pt(2)	0.1646	0.1500	0.1666
Pt(1)-Ag(1)	−0.0148	0.0432	−0.0292
Pt(2)-Ag(1)	−0.0022	0.0693	−0.0340
Pt(1)-S(1)	0.3115	0.3094	0.3122
Pt(2)-S(1)	0.2944	0.2895	0.2971
Ag(1)-Cl(1)	0.2119	0.2148	0.2105
Ag(1)-S(1)	0.1705	0.1494	0.1903

of the S → Cu electron donation is reflected in a stronger Cu−S bond [2.210(2) Å] compared to those obserbed in $[Pt_2(PPh_3)_4(\mu_3\text{-}S)_2Cu(PPh_3)]PF_6$ [av 2.286(5) Å].[2g] The Cu−Cl bond [2.172-(2) Å] is typically covalent {*e.g.* Cu−Cl: av 2.145(2) Å in $[CuCl(SPMe_3)]_3$[11] }.

Preparation and Characterization of $[Pt_2(CO)_2(PPh_3)_2(\mu_3\text{-}S)RuCl(CO)(PPh_3)]Cl$ (8). To demonstrate that this cluster synthesis is applicable to a system outside the coinage metals, we have synthesized **8** from $[Pt_2(PPh_3)_4(\mu_3\text{-}S)_2RuCl(PPh_3)_2]Cl$ (**7**), which is isolated from **1** and $RuCl_2(PPh_3)_3$ (Scheme 3). Conductivity measurement shows **8** to be a 1:1 electrolyte. The Pt carbonyl absorptions occur at 2077 (m) and 2034 (s) cm^{-1} whereas the Ru carbonyl absorption occurs at 1966 (m) cm^{-1}. The heterometal attachment promotes S → Ru donation and shifts the electron density away from the Pt_2 core. This is verified by the high-energy shift of the carbonyl absorptions as compared to the parent $Pt_2(CO)_2(PPh_3)_2(\mu\text{-}S)$ (ν_{CO} 2027 and 1990 cm^{-1}).[2f] The presence of three chemically distinct carbonyls and phosphines is verified by the distinctive resonances in the ^{13}C and $^{31}P\{^1H\}$ NMR spectra. Cluster **8** is not stable as exemplified by its gradual decomposition by CO dissociation.

(11) Tiethof, J. A.; Stalick, J. K.; Meek, D. W. *Inorg. Chem.* **1973**, *12*, 1170.

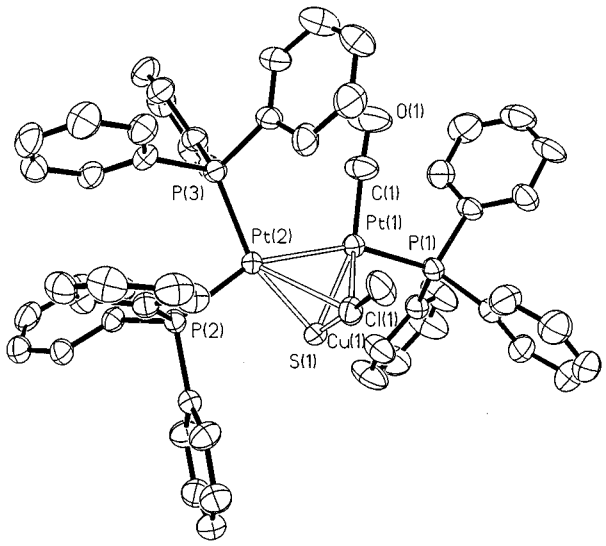

Figure 4. An ORTEP plot of $[Pt_2(CO)(PPh_3)_3(\mu_3\text{-}S)CuCl]$, **6**, with a 50% probability level.

Table 4. Selected Bond Lengths (Å) and Angles (deg) in $[Pt_2(CO)(PPh_3)_3(\mu_3\text{-}S)CuCl]$ (**6**)

Pt(1)−Pt(2)	2.657(1)	Cu(1)−Pt(1)	2.888(1)
Cu(1)−Pt(2)	2.755(1)	Pt(1)−S(1)	2.285(2)
Pt(2)−S(1)	2.288(2)	Cu(1)−S(1)	2.210(2)
Pt(1)−P(1)	2.316(2)	Pt(2)−P(2)	2.276(2)
Pt(2)−P(3)	2.262(2)	Pt(1)−C(1)	1.842(9)
Cu(1)−Cl(1)	2.172(2)	C(1)−O(1)	1.154(12)
Pt(1)−Pt(2)−Cu(1)	64.2(1)	Pt(1)−Cu(1)−Pt(2)	55.9(1)
Pt(2)−Pt(1)−Cu(1)	59.9(1)	Pt(1)−Pt(2)−S(1)	54.4(1)
Pt(1)−S(1)−Pt(2)	71.0(1)	Pt(2)−Pt(1)−S(1)	54.5(1)
Pt(1)−Cu(1)−S(1)	51.2(1)	Pt(1)−S(1)−Cu(1)	79.9(1)
Cu(1)−Pt(1)−S(1)	48.9(1)	Pt(2)−Cu(1)−S(1)	53.2(1)
Pt(2)−S(1)−Cu(1)	76.2(1)	Cu(1)−Pt(2)−S(1)	50.7(1)
Pt(1)−Cu(1)−Cl(1)	132.0(1)	Pt(2)−Cu(1)−Cl(1)	124.2(1)
Cl(1)−Cu(1)−S(1)	175.1(1)	Pt(1)−Pt(2)−P(2)	154.2(1)
Pt(1)−Pt(2)−P(3)	103.6(1)	Pt(2)−Pt(1)−P(1)	157.0(1)
Pt(2)−Pt(1)−C(1)	104.7(3)	Cu(1)−Pt(1)−C(1)	122.0(3)
Cu(1)−Pt(1)−P(1)	110.5(1)	Cu(1)−Pt(2)−P(2)	101.8(1)
Cu(1)−Pt(2)−P(3)	125.0(1)	P(1)−Pt(1)−C(1)	97.9(3)
P(2)−Pt(2)−P(3)	102.2(1)	Pt(1)−C(1)−O(1)	176.7(10)

Conclusion. Although the $[Pt_2(CO)(PPh_3)_3(\mu_3\text{-}S)M(PPh_3)]^+$ (M = Ag, Cu) clusters can be easily assembled from an addition reaction between the heterometallic fragments of $[Pt_2(CO)(PPh_3)_3(\mu\text{-}S)]$ and $[M(PPh_3)]^+$,[8] they cannot be accessed by a similar reductive carbonylation of $[Pt_2(PPh_3)_4(\mu_3\text{-}S)_2Ag(PPh_3)]^+X^-$

Scheme 3

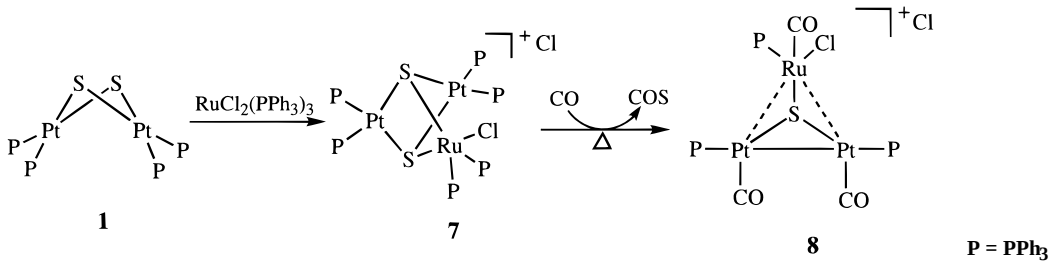

1 **7** **8**

Table 5. Summary of Crystallographic Data for the Structures of **2b**(**A**), **2b**(**B**), **4**, and **6**

	2b			
	polymorph **A**	polymorph **B**	**4**	**6**
formula	$C_{90}H_{75}AgF_6P_6Pt_2S_2$	$C_{90}H_{75}AgF_6P_6Pt_2S_2$	$C_{55}H_{45}AgClOP_3Pt_2S$	$C_{55}H_{45}ClCuOP_3Pt_2S$
fw	2018.5	2018.5	1379.4	1336.0
crystal size, mm	0.20 × 0.40 × 0.40	0.10 × 0.12 × 0.22	0.13 × 0.30 × 0.40	0.18 × 0.22 × 0.36
space group	$P2_12_12_1$ (No. 19)	$P\bar{1}$ (No. 2)	$P2_1/n$ (No. 14)	$P2_1/n$ (No. 14)
a, Å	14.229(1)	14.934(1)	12.010(2)	11.932(1)
b, Å	18.674(1)	15.039(1)	30.195(6)	30.210(2)
c, Å	30.127(1)	19.744(1)	13.897(3)	13.946(1)
α, deg		74.55(1)		
β, deg		88.01(1)	91.62(3)	91.36(1)
Γ, deg		79.88(1)		
V, Å^3	8005(2)	4207(1)	5038(3)	5026(3)
Z	4	2	4	4
D_c, g/cm^3	1.675	1.593	1.819	1.766
μ, mm^{-1}	3.96	3.77	6.153	6.20
radiation, Å	0.71073	0.71073	0.71073	0.71073
temp, K	150	150	298	298
2θ range, deg	3.0−61.8	3.0−61.3	7.0−45.0	7.0−45.0
no. of ind	22576	22404	10766	11541
no. of obsd	21110 [$F_o \geq 4\sigma(F_o)$]	14510 [$F_o \geq 4\sigma(F_o)$]	7511 [$F > 3.0\sigma(F)$]	7739 [$\|F_o\| \geq 4\sigma(\|F_o\|)$]
no. of variables	966	934	577	578
R	0.026	0.063	0.043	0.040
R_w[a]	0.050	0.142	0.050	0.045

[a] Weighting scheme for **2b**(**A**): $w^{-1} = [\sigma^2(F) + (0.0089P)^2 + 10.85P]$, $P = [\max(F_o^2, \theta) + 2F_c^2]/3$. For **2b**(**B**): $w^{-1} = [\sigma^2(F) + (0.0720P)^2 + 3.74P]$, $P = [\max(F_o^2, \theta) + 2F_c^2]/3$. For **4**: $w^{-1} = \sigma^2(F) + 0.0018F^2$. For **6**: $w^{-1} = \sigma^2(F) + 0.0002F^2$.

(X = PF_6, NO_3) or the Cu analogues. Under forcing conditions, *e.g.*, when a high CO pressure and temperature is used, deheterometalation would take place resulting in [Pt_2(CO)-(PPh_3)$_3$(μ-S)]. This shows a stabilizing role played by chloride on the heterometal, which strengthens the M−S and M−Pt bonds and ensures the survival of the heterometallic clusters. We shall explore the influence of other peripheral ligands on the cluster stability in our future work.

Experimental Section

General Consideration. All reactions carried out in CO atmosphere were performed in a stainless-steel bomb cylinder of an autoclave (Parr T316ss reactor with a magnetic drive). All solvents were distilled and deoxygenated by argon before use. Complex **1** was synthesized from *cis*-[$PtCl_2(PPh_3)_2$] and $Na_2S\cdot 9H_2O$ according to the literature method.[12] Elemental analyses were carried out in the Microanalytical Laboratory in our department in the National University of Singapore (NUS). $^{31}P\{^1H\}$ NMR and ^{13}C NMR spectra were run on a Bruker ACF 300 spectrometer at 298 K. IR spectra were taken in a KBr disk on a Perkin-Elmer 1600 FT-IR spectrophotometer. Solution conductivity was measured by using a STEM Conductivity 1000 meter.

Preparation of [Pt_2(CO)(PPh_3)$_3$(μ_3-S)AgCl] (4). A suspension of complex **1** (0.15 g, 0.1 mmol) and AgCl(PPh_3) (0.040 g, 0.1 mmol) in THF (40 mL) was flushed with CO and stirred in an autoclave for 24 h at 80 °C under a CO pressure of 60 psi. The liberation of COS gas was verified by the formation of a white precipitate upon passing the residual gas through a clear solution of $Ca(OH)_2$. The resultant clear orange solution was added to hexane (60 mL) after which the orange precipitate, which contains some unknown platinum compounds, was filtered off. The filtrate was evaporated to dryness under vacuum. The residue was recrystallized from CH_2Cl_2/hexane to give **4**. The product was further purified by dissolving the sample in CH_2Cl_2/MeOH (1:3, 10 mL), filtering the resulting solution, and evaporating the filtrate slowly in air to give orange crystals of **4** (0.049 g, 36%). Anal. Calcd for $C_{55}H_{44}AgClOP_3Pt_2S$: C, 47.8; H, 3.2; P, 6.7; S, 2.3. Found: C, 47.0; H, 3.2; P, 6.6; S, 2.5. IR: ν(CO) 2025 cm^{-1} (s). $^{31}P\{^1H\}$ NMR ($CDCl_3$) $\delta_{P(1)}$ 16.4, $\delta_{P(2)}$ 18.1, $\delta_{P(3)}$ 20.1 [$^1J_{P(1)-Pt}$ = 2672 Hz, $^1J_{P(2)-Pt}$ = 3326 Hz, $^1J_{P(3)-Pt}$ = 3886 Hz; $^2J_{P(1)-Pt}$ = 184 Hz, $^2J_{P(3)-Pt}$ = 192 Hz; $^3J_{P(1)-P(2)}$ = 16 Hz, $^3J_{P(1)-P(3)}$ = 23 Hz] [the assignments of P(1), P(2), and P(3) are indicated in Figure 3]. Λ_m (10^{-3} M, acetone) 10.7 ohm^{-1} cm^2 mol^{-1}.Cluster **4** was also prepared from [$Pt_2(PPh_3)_4(\mu_3\text{-}S)_2Ag(PPh_3)$]-Cl (**2a**)[2h] (0.192 g, 0.1 mmol) and CO in THF under similar conditions (yield 0.055 g, 40%).

Preparation of [Pt_2(CO)(PPh_3)$_3$(μ_3-S)CuCl] (6). Cluster **6** was prepared by a similar procedure by using **1** (0.15 g, 0.1 mmol) and CuCl (0.010 g, 0.1 mmol) in THF (40 mL) (yield 0.043 g, 32%). Anal. Calcd for $C_{55}H_{44}CuClOP_3Pt_2S$: C, 49.4; H, 3.3; P, 7.0; S, 2.4. Found: C, 49.0; H, 3.3; P, 6.8; S, 2.6. IR: ν(CO) 2026 cm^{-1} (s). $^{31}P\{1H\}$ NMR ($CDCl_3$): $\delta_{P(1)}$ 16.3, $\delta_{P(2)}$ 19.4, $\delta_{P(3)}$ 18.0 [$^1J_{P(1)-Pt}$ = 2660 Hz, $^1J_{P(2)-Pt}$ = 3808 Hz; $^1J_{P(3)-Pt}$ = 3322 Hz, $^2J_{P(1)-Pt}$ = 185 Hz, $^2J_{P(3)-Pt}$ = 200 Hz; $^3J_{P(1)-P(2)}$ = 15 Hz, $^3J_{P(1)-P(3)}$ = 21 Hz] [the labeling of P(1), P(2), and P(3) is indicated in Figure 4].

Preparation of [$Pt_2(PPh_3)_4(\mu_3\text{-}S)_2RuCl(PPh_3)_2$]Cl (7). To a THF solution (50 mL) of $RuCl_2(PPh_3)_3$ (0.096 g, 0.1 mmol) was added **1** (0.15 g, 0.1 mmol) under argon. The suspension dissolved after 4 h of stirring in a water bath (∼50 °C) to give a clear dark brown solution. The solution was filtered under argon and the filtrate was evaporated in *vacuo* to *ca*. 10 mL. Addition of hexane gave rise to a brown precipitate, which was isolated by filtration and purified by recrystallization from CH_2Cl_2/hexane to yield **7** (0.121 g, 55%). Anal. Calcd

(12) Ugo, R.; La Monica, G.; Cenini, S.; Segre, A.; Conti, F. *J. Chem. Soc. A* **1971**, 522.

for $C_{108}H_{90}Cl_2P_6Pt_2RuS_2$: C, 59.0; H, 4.1; Cl, 3.2; S, 2.9. Found: C, 58.0; H, 4.0; Cl, 3.2; S, 2.2. Λ_m (10^{-3} M, MeOH) 76.8 ohm^{-1} cm^2 mol^{-1}. ^{31}P{1H} NMR ($CDCl_3$): δ 29.2 (2P, s), 14.3 (4P, t, ^1J(P−Pt) = 3674 Hz).

Preparation of [Pt$_2$(CO)$_2$(PPh$_3$)$_2$(μ_3-S)RuCl(CO)(PPh$_3$)]Cl (8). Complex **8** was prepared in a manner analogous to **4** by using **7** (0.110 g, 0.05 mmol) in THF (40 mL) (yield 0.027 g, 37%). Anal. Calcd for $C_{57}H_{45}Cl_2O_3P_6Pt_2RuS$: C, 46.7; H, 3.1; Cl, 4.8; P, 6.4; S, 2.2. Found: C, 47.3; H, 3.2; Cl, 4.5; P, 5.8; S, 2.9. Λ_m (10^{-3} M, MeOH) 69.1 ohm^{-1} cm^2 mol^{-1}. ^{31}P{^{1}H} NMR ($CDCl_3$): δ 14.9 (P, t, ^1J(P−Pt) = 3220 Hz), 13.0 (P, t, ^1J(P−Pt) = 3198 Hz), 9.0 (1P, s). ^{13}C NMR ($CDCl_3$): δ 194.2 (1C, s), 194 (1C, s), and 193.9 (1C, s). IR: ν(CO) 2077 (m), 2034 (s), and 1996 (m) cm^{-1}.

X-ray Crystal Structure Studies. Single crystals of **2b**, **4**, and **6** suitable for X-ray diffraction studies were grown from CH_2Cl_2/MeOH solutions by slow evaporation at room temperature in air. Data collections of the two polymorphic modifications of **2b** were carried out on a Siemens CCD SMART system, while a Siemens R3m/v diffractometer was used for **4** and a Rigaku AFC7 diffractometer was used for **6**. Details of crystal and data collection parameters are summarized in Table 5.

The structures of both modifications of **2b**, **4**, and **6** were solved by direct methods and difference Fourier maps. Full-matrix least-squares refinement was carried out with the anisotropic temperature factor for all non-hydrogen atoms. Hydrogen atoms were placed on calculated positions (C−H 0.96 Å) and assigned isotropic thermal parameters riding on their parent atoms. Initial calculations were carried out on a PC with the SHELXTL PC software package; SHELXTL-93[13] was used for the final refinement.

Acknowledgment. We acknowledge the support by the National University of Singapore (NUS) (RP 950695). H. L. thanks NUS for a research scholarship. A. L. T. thanks the National Science and Technology Board for a postdoctoral fellowship, and the National Supercomputing Research Centre for use of its computing facilities and software.

Supporting Information Available: Tables of crystal data, atomic coordinates, bond distances and angles, and anisotropic thermal parameters (42 pages). See any current masthead page for ordering and Internet access instructions.

JA9718376

(13) Sheldrick, G. M. *SHELXL-93, Program for Crystal Structure Refinement*; University of Göttingen, Germany, 1993.